Conductance, contacts, and interface states in single alkanedithiol molecular junctions

Chao-Cheng Kaun* and Tamar Seideman†
Department of Chemistry, Northwestern University, 2145 Sheridan Road, Evanston, Illinois 60208-3113, USA
(Received 4 November 2006; revised manuscript received 31 May 2007; published 23 January 2008)

We calculate the conductance of Au-alkanedithiol-Au molecular junctions from first principles, finding agreement with measured data [B. Xu and N. J. Tao, Science **301**, 1221 (2003)] for junctions where the terminal S atoms are attached to top sites of the gold electrodes. A major effect of the contact geometry on the conduction properties is found, whose origin is traced to the symmetry and spatial localization of the interface states. The implications of our finding to ongoing experiments are noted.

DOI: 10.1103/PhysRevB.77.033414 PACS number(s): 73.63.−b, 73.43.Cd, 73.20.−r, 73.43.Jn

The challenge of understanding the charge transport properties of molecular-scale electronic devices has inspired a considerable amount of experimental and theoretical research in recent years, leading to the development of new fundamental concepts along with intriguing potential applications.[1] One of the important objectives of this research has been the quantitative comparison of measured and computed conductance through single-molecule junctions. While the difficulty is obvious, such comparison could bring the research on molecular conductance to a next level, enabling direct theoretical analysis of experimentally observed phenomena as well as numerical design of realistic devices.

It is for this reason that the experiments of Xu and Tao, reported in Ref. 2, have led to substantial theoretical and experimental activity.[3–12] By choosing a relatively simple molecular junction, namely, the Au-alkanedithiol-Au construct, where resonant conductance and current-driven events play no role, and by repeating the measurement using thousands of junctions to allow statistical determination, Ref. 2 introduced an opportunity for theoretical research. Theoretical studies addressed this challenge through application of different numerical approaches, leading to the sought enhancement of our understanding of the transport through molecular junctions.[3–7] Interestingly, several recent experiments[8–10] disagree with the results of Ref. 2. Consistent results that are five times smaller than the conductance of Ref. 2 have been reported in Refs. 11 and 12. Reference 11 attributed the discrepancy to structural differences.

Our goal in the present contribution is to first model the results of Ref. 2 using state of the art numerical methods and next inquire into effects that may give rise to marked discrepancies among high-quality measurements, even for relatively understood molecular junctions. We use a nonequilibrium Green's function[13,14] (NEGF) approach with a density functional theory Hamiltonian, allowing the calculation of the charge density without phenomenological parameters.[15–20] The method has been used by several groups for a variety of applications and is well documented. In brief, the charge density is computed within the Keldysh NEGF theory, taking into account the open system boundary conditions via an iterative procedure. Once the Kohn-Sham effective potential has been self-consistently converged, the transport properties of the device are calculated. The present application expands the Hamiltonian in a real space s,p,d double zeta plus polarization (DZP) atomic orbital basis set, using the software packages TRANSIESTAC (Ref. 21) and MCDCAL.[15] [The discussion below also notes briefly the results of calculations at the single zeta plus polarization (SZP) level.] The atomic cores are defined by standard, nonlocal, and norm-conserving pseudopotentials.[22] The local density approximation is used for the description of electron exchange and correlation.[26]

We first consider the device model shown in Fig. 1(a), where an alkanedithiol molecule is connected to the top sites of two gold electrodes extending to infinity in the $\pm z$ directions. The molecular junction geometry was optimized by initially optimizing the geometry of a subsystem consisting of the molecular moiety connected to two Au_5 clusters through the terminal S atoms.[27] The Au clusters were constructed to mimic the top layers of the gold electrodes, with one layer of four Au atoms spatially fixed and forming the base of a pyramid and a fifth Au atom (forming the pyramid tip) attached to the S atom. The distance between the bases of the two Au pyramids was fixed at 17.539 Å (the largest of the values for which the junction has been optimized). We next placed the optimized Au_5-alkanedithiol-Au_5 construct in the gap between two gold electrodes composed of unit cells with 18 Au atoms (four layers) oriented in the (100) direction, repeated to $z=\pm\infty$.[28] In the minimum energy configuration, the molecule and the junction are almost coaxial, see Fig. 1(a). The scattering region indicated by a square in Fig.

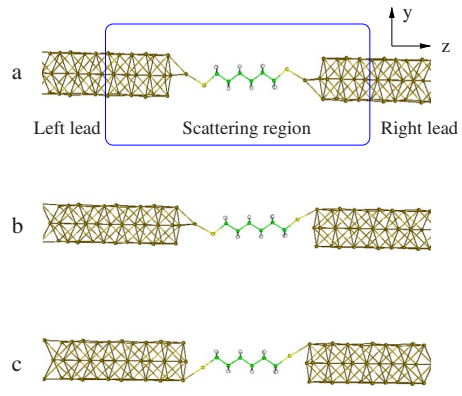

FIG. 1. (Color online) Schematic illustration of the Au-alkanedithiol-Au junctions. Three device contacts are studied, where the thiol groups are attached to (a) top sites, (b) one hollow and one top site, and (c) hollow sites. The scattering region forming our simulation box, which includes a portion of the infinitely long electrodes and the alkanedithiol molecule, is indicated in (a).

1(a) forms our simulation box. Using the NEGF approach with a DZP basis set, we calculated the conductance at zero bias for junctions of hexanedithiol, octanedithiol, and decanedithiol, finding $0.0018G_0$, $0.000\,26G_0$, and $0.000\,04G_0$, respectively, where $G_0=2e^2/h$ is the conductance quantum. As a test of the sensitivity of the conductance to the quality of the basis set, we repeated the calculation with a SZP basis set, finding $0.0011G_0$, $0.000\,13G_0$, and $0.000\,02G_0$ for junctions of hexanedithiol, octanedithiol, and decanedithiol, respectively. Our results are thus in good agreement with the measured data ($0.0012G_0$, $0.000\,25G_0$, and $0.000\,02G_0$ for the hexanedithiol, octanedithiol, and decanedithiol, respectively[2]), suggesting that the calculated configurations used in our transport studies could correspond to the structures in the measurements of Ref. 2.

An interesting question is thus what could lead to the fivefold smaller conductance observed in Refs. 11 and 12 as compared with the data of Ref. 2. A plausible answer could be provided by investigating the extent to which small variations in the contact geometry may modify the conductance. Under different tip retracting speeds, system temperatures, environment impurities, or junction currents, the contact optimized geometry could differ. We therefore repeated the calculation with the rightmost S atom attached in the hollow configuration, leaving the left contact attached to the top configuration, Fig. 1(b). In order to focus on the role of the contact site, we left all other structural parameters as in the junction of panel (a) (rather than reoptimizing the structure) and fixed the distance between the sulfur atom and the surface of the Au lead at 4.0 a.u. (roughly the equilibrium bond length determined in Ref. 32). The calculated conductance of hexanedithiol junction in this configuration increases to $0.0045G_0$ with the DZP basis ($0.0029G_0$ using the SZP basis). We then changed both thiol ends to attach to the electrodes at the hollow sites (keeping the contact distance at 4.0 a.u.), as shown in Fig. 1(c). With this configuration, the junction conductance increases to $0.0073G_0$ with the DZP basis (to $0.0051G_0$ with the SZP basis).

It is important to restress that our thrust is not to verify one experiment or question another since the experimental parameters are not known with sufficient details. In particular, we do not expect that the junctions of Figs. 1(b) and 1(c) reproduce precisely the geometry of the junctions probed in any of the recent experiments on the Au-alkane-Au problem, Refs. 8–12. Our calculations do, however, point to the dramatic sensitivity of the conductance to the fine details of the contact geometry, which would make comparison of measurements conducted in different laboratories difficult at best.

We proceed to unravel the origin of the marked sensitivity of the transport properties to the contact site. To that end, in Fig. 2, we plot the transmission spectra $T(E)$ and the molecular energy levels of the Au-hexanedithiol-Au junction for the three different contact geometries of Fig. 1. The Fermi energy of the junction defines the zero of energy, $E_F=0$. The molecular levels are computed by diagonalizing the sub-Hamiltonian that includes all the atoms in the scattering region of Fig. 1(a), corresponding to an extended system Hamiltonian. We focus on the eigenfunctions that are spatially delocalized, since these are predominantly responsible for electron tunneling through the junction and, hence, their properties are most relevant for interpretation of the transmission spectra.

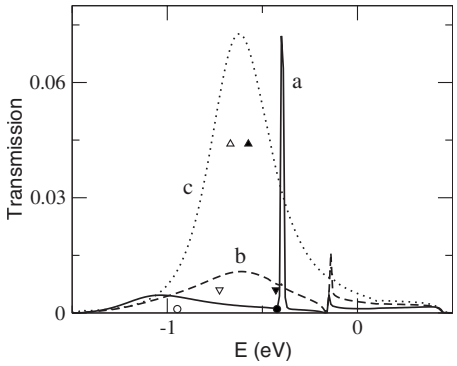

FIG. 2. Transmission spectra $T(E)$ and molecular energy levels for the alkanedithiol junctions of Fig. 1. The solid curve marked "a" and the circles correspond to the junction of Fig. 1(a), the dashed curve marked "b" and the triangles pointing down correspond to the junction of Fig. 1(b), and the dotted curve marked "c" along with the triangles pointing up correspond to the junction of Fig. 1(c). The Fermi level defines the zero of energy, $E_F=0$.

The solid curve marked "a" in Fig. 2 shows the transmission through the junction of Fig. 1(a), where both terminal S atoms attach to the top sites. The spectrum exhibits large transmission peaks at approximately −1.04 and −0.40 eV, which arise from tunneling via the molecular levels indicated by empty and solid circles, respectively. The dashed curve marked "b" shows the transmission through the junction of Fig. 1(b), where one terminal S atom attaches to the top site and the other to the hollow site. The major transmission peak, located at −0.61 eV, arises from tunneling via the molecular levels indicated by empty and solid triangles pointing down. The dotted curve marked "c" shows the transmission through the junction of Fig. 1(c), where both terminal S atoms attach to hollow sites. The major transmission peak, located at −0.62 eV, results from tunneling via the molecular levels indicated by empty and solid triangles pointing up. The small transmission peaks at −0.2 eV are attributed to the presence of a band edge. Clearly, the major transmission peak of the configuration of Fig. 1(a) is a long-lived resonance that is poorly coupled to the continua and has vanishingly small amplitude at the Fermi energy. By contrast, the junction of Fig. 1(c) supports a broad feature of decay rate $\Gamma=\hbar/\tau\approx 0.38$ eV and significant amplitude at E_F, hence the nearly fivefold increase in the conductivity of this junction compared to that of Fig. 1(a).

We proceed to explore the origin of the large difference between the transmission spectra of the three junctions. Figure 3 shows the real part of the junction interface wave functions whose energy positions are indicated in Fig. 2. The symbols in Fig. 3 associate each function with its energy location and its role in the transmission in Fig. 2. These functions determine the junction conductance by controlling the effective tunneling distance. [We provide in the supplementary material section figures that show the spatial localization and symmetry of the eigenstates of a truncated Hamiltonian, corresponding to a subsystem that contains only the molecule and the clusters of either four or five Au

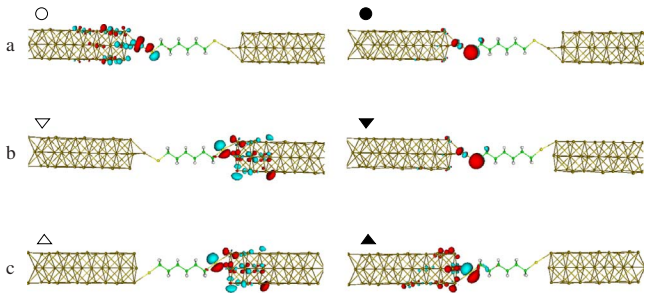

FIG. 3. (Color online) The real part of the interface wave function for the molecular junctions of Fig. 1. Panels (a), (b), and (c) correspond to panels (a), (b), and (c) of Fig. 1 and to curves a, b, and c of Fig. 2.

atoms that form the edges of the two electrodes. These functions contain less of the transmission physics (the corresponding eigenvalues are shifted with respect to the transmission peaks) but are more intuitive in form, as they are dominated by the molecular moiety.] Figure 3(a), corresponding to the transmission curve marked by "a" in Fig. 2 and to the junction of Fig. 1(a), illustrates the dominant effect of the terminal Au atom on the interface interaction when the S atom is attached at the top site. The interface wave function, indicated by an empty circle, is mainly composed of orbitals from the Au electrode, the d_{z^2} orbital of the terminal Au atom, and the p_z and p_y orbitals of the S atom. The propagating Bloch wave through the junction is from a band of the Au electrode that has s, p_z, and d_{z^2} character. On the other hand, the function indicated by the solid circle is mainly composed of the d_{xy} orbital of the terminal Au atom, the p_x orbitals of the S atom, and the p_x orbitals of the alkyl part. The propagating Bloch wave here is from the d_{xy}-character band of the Au electrode. Consequently, this function contributes little to the conductance through the junction. The same conclusion is readily drawn from Fig. 3(a), which illustrates the spatial localization of the (real part of the) wave function in a plane containing the junction axis.

Figure 3(b) corresponds to the transmission curve marked by "b" in Fig. 2 and to the junction of Fig. 1(b). Here, the function indicated by an empty triangle pointing down is mainly composed of orbitals from the Au electrode and the p_z and p_y orbitals of the S atom. Transport of electrons is from the s, p_z, d_{z^2}-character band. The availability of spatially delocalized interface states gives rise to the computed enhanced conductivity compared to that of the junction of panel (a). The function indicated by the solid triangle pointing down is similar to the one indicated by solid circle in Fig. 3(a). Since, however, there is no extruding Au atom in the right electrode to resonate the electrons from the d_{xy} band, this level does not give rise to a sharp transmission peak. Finally, in the case of Fig. 3(c), the function indicated by an empty triangle pointing up is similar in character to the one indicated by an empty triangle pointing down in Fig. 3(b). The function indicated by a solid triangle pointing up is mainly composed of orbitals from the Au electrode, the p_z and p_y orbitals of the S atom, and the p_z and p_y orbitals of the alkyl part (along the σ bond). Transport of electrons through both functions in this configuration is from the s, p_z, d_{z^2}-character band. Of the three junctions considered, this corresponds to the best delocalization in space along the junction axis, and hence to the highest conductance.

In summary, our first-principles calculations of the conductance of Au-alkanedithiol-Au junctions are in good agreement with the experimental data of Ref. 2, pointing, however, to marked sensitivity of the conductance to the contact geometry. This feature is explained in terms of the symmetry and spatial delocalization of the underlying molecular orbitals. Our results illustrate that conductance experiments provide a sensitive probe of the interface interactions that play a key role in molecular-scale electronics.

We thank M. A. Ratner for fruitful discussions and the NSF (Grant No. CHEM/MRD-0313638) for generous support.

*Present address: Research Center for Applied Sciences, Academia Sinica, Taipei 11529, Taiwan, Republic of China.
†Author to whom correspondence should be addressed; t-seideman@northwestern.edu

[1] See, for instance, L. Venkataraman, J. E. Klare, C. Nuckolls, M. S. Hybertsen, and M. L. Steigerwald, Nature (London) **442**, 904 (2006); M. Lefenfeldt, J. Baumert, E. Sloutskin, I. Kuzmenko, P. Pershan, M. Deutsch, C. Nuckolls, and B. M. Ocko, Proc. Natl. Acad. Sci. U.S.A. **103**, 2541 (2006); C. Joachim and M. A. Ratner, *ibid.* **102**, 8801 (2005); H. Ness and A. J. Fisher, *ibid.* **102**, 8826 (2005); J. G. Kushmerick, S. K. Pollack, J. C. Yang, J. Naciri, D. B. Holt, M. A. Ratner, and R. Shashidhar, Ann. N.Y. Acad. Sci. **1006**, 277 (2003); M. Ouyang, J. L. Huang, C. L. Cheung, and C. M. Lieber, Science **291**, 97 (2001).
[2] B. Xu and N. J. Tao, Science **301**, 1221 (2003).
[3] Y. Hu, Y. Zhu, H. Gao, and H. Guo, Phys. Rev. Lett. **95**, 156803 (2005).
[4] K.-H. Muller, Phys. Rev. B **73**, 045403 (2006).
[5] Z. Ning, J. Chen, S. Hou, J. Zhang, Z. Liang, J. Zhang, and R. Han, Phys. Rev. B **72**, 155403 (2005).
[6] H. Basch, R. Cohen, and M. A. Ratner, Nano Lett. **5**, 1668 (2005).
[7] T. Tada, M. Kondo, and K. J. Yoshizawa, Chem. Phys. **121**, 8050 (2004).
[8] W. Haiss, R. J. Nichols, H. Zalinge, S. J. Higgins, D. Bethell, and D. J. Schiffrin, Phys. Chem. Chem. Phys. **6**, 4330 (2004).
[9] J. Ulrich, D. Esrail, W. Pontius, L. Venkataraman, D. Millar, and L. H. Doerrer, J. Phys. Chem. B **110**, 2462 (2006).
[10] L. Venkataraman, J. E. Klare, I. W. Tam, C. Nuckolls, M. S. Hybertsen, and M. L. Steigerwald, Nano Lett. **6**, 458 (2006).
[11] X. Li, J. He, J. Hihath, B. Xu, S. M. Lindsay, and N. J. Tao, J. Am. Chem. Soc. **128**, 2135 (2006).
[12] S.-Y. Jang, P. Reddy, A. Majumdar, and R. A. Segalman, Nano Lett. **6**, 2362 (2006).

[13] S. Datta, *Electronic Transport in Mesoscopic Systems* (Cambridge University Press, New York, 1995).
[14] A. P. Jauho, N. S. Wingreen, and Y. Meir, Phys. Rev. B **50**, 5528 (1994).
[15] J. Taylor, H. Guo, and J. Wang, Phys. Rev. B **63**, 245407 (2001).
[16] T. Seideman and H. Guo, J. Theor. Comput. Chem. **2**, 439 (2003).
[17] M. Brandbyge, J.-L. Mozos, P. Ordejon, J. Taylor, and K. Stokbro, Phys. Rev. B **65**, 165401 (2002).
[18] P. S. Damle, A. W. Ghosh, and S. Datta, Phys. Rev. B **64**, 201403(R) (2001).
[19] Y. Xue, S. Datta, and M. A. Ratner, Chem. Phys. **281**, 151 (2002).
[20] S.-H. Ke, H. U. Baranger, and W. Yang, Phys. Rev. B **70**, 085410 (2004).
[21] TRANSIESTAC is provided by Atomistix Inc. (www.atomistix.com).
[22] TRANSIESTAC uses the Troullier-Martins (Ref. 23) pseudopotentials whereas MCDCAL uses the Hamann-Schluter-Chiang (Refs. 24 and 25) pseudopotentials.
[23] N. Troullier and J. L. Martins, Phys. Rev. B **43**, 1993 (1991).
[24] D. R. Hamann, M. Schluter, and C. Chiang, Phys. Rev. Lett. **43**, 1494 (1979).
[25] G. B. Bachelet, D. R. Hamann, and M. Schluter, Phys. Rev. B **26**, 4199 (1982).
[26] The local density approximation is known to fail to describe the band gap. In the molecules considered in the present study, however, the lowest unoccupied molecular orbital is remote from the Fermi level (about 8 eV, while the band gap is ~11 eV), and thus plays little role on conductance.
[27] JAGUAR 5.5, Schrödinger, L. L. C., Portland, OR, 1991–2003.
[28] Although the experimental electrode geometry is not known, experimental and numerical results (Refs. 2 and 29–31) suggest that the conductance in the scenarios considered here is best modeled by a gold nanowire. As a scanning tunneling microscope tip is gradually retracted from contact with a gold substrate, a nanowire forms at the contact (the narrowest part of the electrode). The single atom chain nature of the wire and the fact that this nanowire dominates the conductance of the junction are evidenced by the observation of quantized conductance (Refs. 2 and 29). Simulations of the formation mechanisms of such atomically thin Au nanowires are provided, e.g., in Ref. 30.
[29] H. Ohnishi, Y. Kondo, and K. Takayanagi, Nature (London) **395**, 780 (1998).
[30] M. R. Sorensen, M. Brandbyge, and K. W. Jacobsen, Phys. Rev. B **57**, 3283 (1998); E. Z. da Silva, Antonio J. R. da Silva, and A. Fazzio, Phys. Rev. Lett. **87**, 256102 (2001).
[31] E. Tosatti, S. Prestipino, S. Kostlmeier, A. Dal Corso, and F. D. Di Tolla, Science **291**, 288 (2001).
[32] D. J. Wold, R. Haag, M. A. Rampi, and C. D. Frisbie, J. Phys. Chem. B **106**, 2813 (2002); H. Sellers, A. Ulman, Y. Shnidman, and J. E. Eilers, J. Am. Chem. Soc. **115**, 9389 (1993).